Optical anisotropy in [0001]-oriented AlxGa1-xN/AlN quantum wells (x > 0.69)

AUTHOR(S):

Banal, R. G.; Funato, M.; Kawakami, Y.

PHYSICAL REVIEW B **79**, 121308(R) (2009)

Optical anisotropy in [0001]-oriented $Al_xGa_{1-x}N/AlN$ quantum wells ($x > 0.69$)

R. G. Banal, M. Funato,* and Y. Kawakami†
Department of Electronic Science and Engineering, Kyoto University, Kyoto 615-8510, Japan
(Received 15 December 2008; revised manuscript received 16 February 2009; published 30 March 2009)

The optical polarization in [0001]-oriented $Al_xGa_{1-x}N/AlN$ multiple quantum wells (QWs) in the deep-ultraviolet region ($x > 0.69$) was studied. Photoluminescence spectroscopy performed at 8.5 K revealed that the predominant polarization direction in QWs with a well width of ~1.5 nm switched from GaN-like $\boldsymbol{E} \perp [0001]$ to AlN-like $\boldsymbol{E} \parallel [0001]$ at an Al composition x of ~0.83, where $\boldsymbol{E}$ is the electric field vector of emitted light. This Al composition is much higher than the previously reported critical compositions for polarization switching phenomena. Furthermore, decreasing the well width from more than 10 to 1.5 nm promoted $\boldsymbol{E} \perp [0001]$ polarization. These results can be explained by the effect of strain and quantum confinement on the valence-band structures.

DOI: 10.1103/PhysRevB.79.121308 PACS number(s): 78.67.De, 73.21.Fg, 78.55.Cr, 81.07.St

Realizing deep-ultraviolet (DUV) semiconductor-based emitters will provide compact, nontoxic, and high-efficiency light sources for various applications, ranging from biological agent detection to next-generation data storage.[1] Although such devices primarily require $Al_xGa_{1-x}N$-based quantum wells (QWs) with a high Al content,[1–5] their fundamental optical properties remain controversial. For example, it has experimentally been demonstrated that surface emissions from [0001]-oriented $Al_{0.66}Ga_{0.34}N/Al_{0.76}Ga_{0.24}N$ QWs (Refs. 3 and 4) and $Al_{0.11}In_{0.03}Ga_{0.86}N/Al_{0.2}In_{0.03}Ga_{0.77}N$ QWs (Ref. 6) are quite weak because of the predominant optical polarization along the [0001] c direction. In contrast, a theoretical study has predicted that valence-band engineering through the well width and/or in-plane compressive strain in c-oriented $Al_xGa_{1-x}N$ QWs may remarkably enhance the emission polarized perpendicular to the c axis,[7] which suggests that surface emitters can be fabricated by better-established growth on the c plane.

Those discussions originate from the valence-band structure in AlN strikingly different from that in conventional GaN. In wurtzite AlN or GaN, the degeneracy of the p-like states at the Γ point is lifted by both crystal-field splitting and spin-orbit splitting, resulting in three valence bands at the Brillouin zone center. Interestingly, AlN has a negative crystal-field splitting energy ($\Delta_{cr} = -217$ meV),[8–12] whereas GaN has a positive Δ_{cr} of 11 meV.[13] These splittings lead to valence-band arrangements in the order of Γ_7, Γ_9, and Γ_7 from the top for AlN, and in the order of Γ_9, Γ_7, and Γ_7 for GaN. The topmost Γ_7 in AlN is the crystal-field split off hole (CH) band governed by p_z-like state, and Γ_9 in GaN is the heavy hole (HH) band governed by p_x-like and p_y-like states. Here, orthogonal coordinates x and y are in the c plane, while $z \parallel c$. Therefore, the emission from high (low) Al-content $Al_xGa_{1-x}N$ is expected to be polarized along (perpendicular to) the c axis. In fact, such a characteristic has been reported for $Al_xGa_{1-x}N$ thick layers; the polarization switches from $\boldsymbol{E} \perp c$ to $\boldsymbol{E} \parallel c$ at $x = 0.25$ as the Al composition (x) increases, where $\boldsymbol{E}$ is the electric field vector of emitted light.[14]

This result implies weak surface emission from c-oriented, Al-rich $Al_xGa_{1-x}N$ QWs, and there are several supporting experimental results as mentioned above.[3,4,6] Then, one may feel that a promising way for strong surface emission from Al-rich $Al_xGa_{1-x}N$ QWs is the growth on non-c planes such as $(1\bar{1}00)$ and $(11\bar{2}0)$, but the growth technology currently remains in its infancy. Herein, the optical polarization anisotropy in Al-rich $Al_xGa_{1-x}N/AlN$ ($x > 0.69$) multiple QWs (MQWs) grown on sapphire (0001) substrates is systematically investigated using photoluminescence (PL) spectroscopy. We demonstrate that the $\boldsymbol{E} \perp c$ polarization of the emission can be achieved up to $x \sim 0.80$, which is even higher than the theoretical prediction.[7] We interpret this observation using a simple model.

After growing ~600-nm-thick high-quality AlN by modified migration-enhanced epitaxy (MEE) (Ref. 15) on sapphire (0001) substrates at 1200 °C, $Al_xGa_{1-x}N/AlN$ MQWs were also fabricated by modified MEE and this time, additional trimethylgallium (TMG) was supplied together with trimethylaluminum (TMA). In addition to controlling the thickness of the barrier and well layers on a per-growth-cycle basis (AlN barriers: 21 cycles and $Al_xGa_{1-x}N$ wells: 1–12 cycles), this method enabled an atomically flat surface to be maintained. The AlN barrier was 13.5 nm thick, and the number of QWs was ten. To increase Ga incorporation into the QWs, the growth temperature was decreased in the range of 1200 and 1060 °C, while maintaining the flow rates of TMG and TMA.

The QW parameters, such as the Al composition, well widths, and barrier widths, were derived from the satellite peaks observed in the x-ray diffraction (XRD) measurements. Reciprocal space mapping by XRD was also performed to confirm the coherent growth of the $Al_xGa_{1-x}N/AlN$ QWs with respect to AlN underlying layers. The optical measurements were carried out at 8.5 K. The excitation source was a pulsed ArF excimer laser ($\lambda = 193$ nm, $\tau = 4$ ns, 25 Hz, and 10 MW/cm^2), which was incident at the surface normal of the samples. PL was collected from the sample edge by one collimating lens and another lens focusing upon the entrance of a 30 cm monochromator (resolution: 0.1 nm). This configuration allowed the polarization PL properties of $\boldsymbol{E} \perp c$ and $\boldsymbol{E} \parallel c$ to be directly assessed using a polarizer inserted between the lenses. The detection was ensured by a liquid-N_2-cooled CCD camera.

To discuss the Al composition dependence of the polarization properties, Fig. 1 shows the PL spectra of a series of

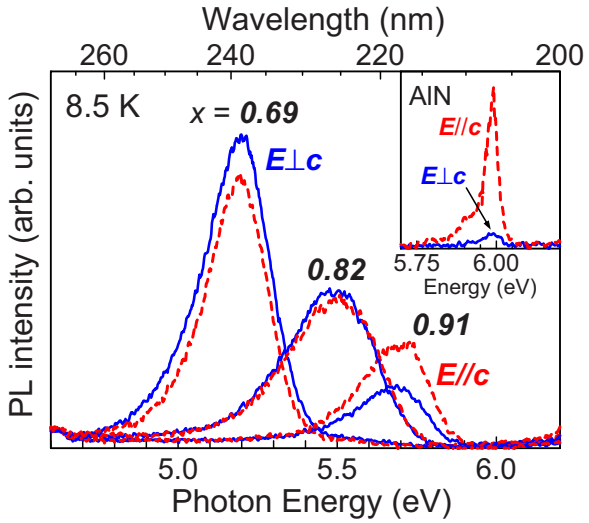

FIG. 1. (Color online) Polarization PL spectra of c-oriented AlN (inset) and $Al_xGa_{1-x}N$ (~1.5 nm)/AlN MQWs with different Al compositions: 0.91, 0.82, and 0.69.

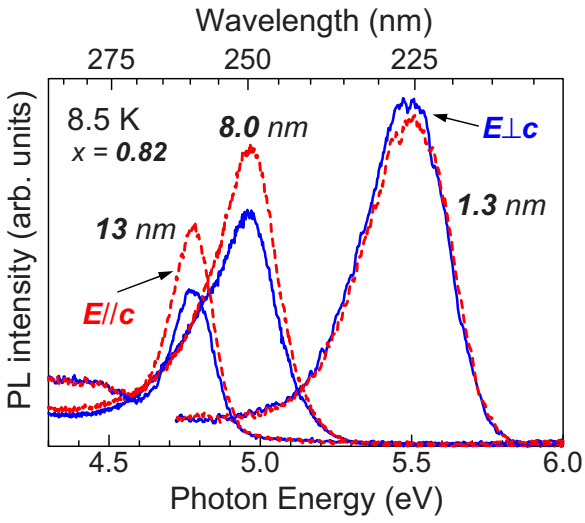

FIG. 2. (Color online) Polarization PL spectra of c-oriented $Al_{0.82}Ga_{0.18}N$/AlN MQWs with different well widths: 1.3, 8.0, and 13 nm.

~1.5-nm-thick $Al_xGa_{1-x}N$/AlN QWs with various Al compositions. The broad line widths were caused by multiple factors such as alloy broadening and inhomogeneous well width, and the detailed PL properties will be discussed elsewhere. The inset shows the polarization PL of AlN used as the template. The calculated polarization degree (ρ) was −0.82, where ρ was defined as $(I_\perp - I_\parallel)/(I_\perp + I_\parallel)$ using the PL intensity perpendicular ($I_\perp$) and parallel ($I_\parallel$) to the c axis. This quantity signifies a strong polarization along the c direction, which is consistent with earlier reports[10–12] and verifies the current experimental setup. For $Al_xGa_{1-x}N$/AlN QWs, as the Al composition decreased from 0.91 to 0.69, the predominant polarization switched from $\boldsymbol{E} \| c$ to $\boldsymbol{E} \perp c$ at $x \sim 0.82$. The polarization degrees (ρ) were evaluated to be −0.24, 0.03, and 0.07 for x=0.91, 0.82, and 0.69, respectively, suggesting a strong surface emission even with x=0.82. In fact, we performed surface emission measurements at 8.5 K for the same series of the QWs and found that the PL intensities of the QWs with x=0.82 and 0.69 increased by factors of 8 and 15, respectively, compared to that of the QW with x=0.91.

The observed polarization switching phenomena suggest that the topmost valence bands of the MQWs change from Γ_7 similar to that in AlN to Γ_9 like that in GaN at $x \sim 0.82$. This Al composition of 0.82 is much higher compared to previous reports,[3,4,6] and the mechanism is discussed below. Here, it should be noted that, because the PL measurements were performed at 8.5 K, majority of photogenerated holes populated the topmost valence band, which dominated the polarization properties observed in this study. The second valence band may influence the PL only when it closely approaches the topmost band. A small peak shift of ~15 meV detectable for the QW with x=0.82 (see Fig. 1) may be due to this effect.

Then the well width dependence of the polarization properties was assessed using $Al_{0.82}Ga_{0.18}N$/AlN MQWs, and the results are shown in Fig. 2. The polarization degrees gradually increased as the QW thickness decreased and were −0.17, −0.12, and 0.03 for QWs with well thicknesses of 13, 8.0, and 1.3 nm, respectively. The emissions from QWs thicker than 8.0 nm showed $\boldsymbol{E} \| c$ polarization, whereas that of the 1.3-nm-thick QW showed $\boldsymbol{E} \perp c$ polarization, indicating that quantum confinement affects the valence-band order and, consequently, promotes $\boldsymbol{E} \perp c$ polarization.

In order to comprehensively understand the polarization properties of $Al_xGa_{1-x}N$/AlN QWs, QWs were then fabricated with various Al compositions and well widths. Figure 3 summarizes the results. As expected, a higher (lower) Al composition resulted in the $\boldsymbol{E} \| c$ ($\boldsymbol{E} \perp c$) polarization. For QWs thicker than ~3 nm, the critical Al composition for the polarization switch was ~0.80 and was independent of the well width. On the other hand, for QWs thinner than ~3 nm, the critical composition shifted toward a higher Al composition, which can be attributed to the quantum confinement effect.

The observed results are closely related to the valence-

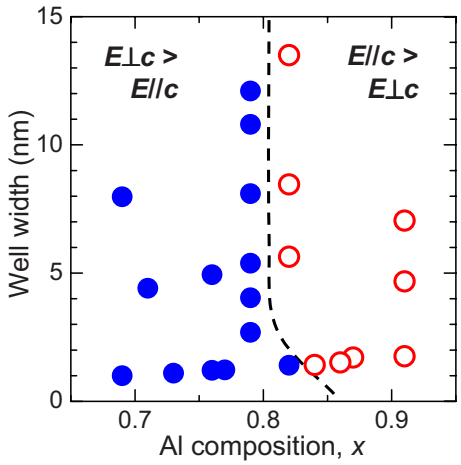

FIG. 3. (Color online) Plot of polarization direction of the emission from $Al_xGa_{1-x}N$/AlN QWs as functions of Al composition and well width.

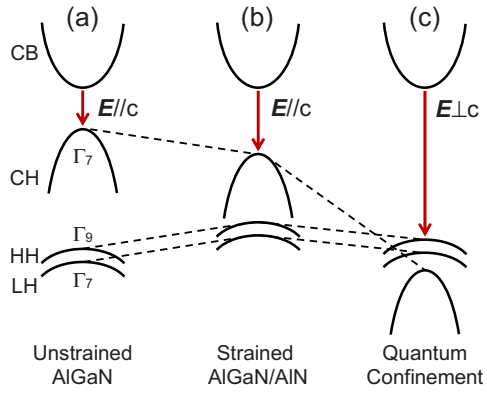

FIG. 4. (Color online) Schematic of band structures for (a) unstrained $Al_xGa_{1-x}N$, (b) strained $Al_xGa_{1-x}N$ on AlN, and (c) $Al_xGa_{1-x}N/AlN$ QWs near the Γ point. CB and LH denote the conduction band and light hole band, respectively.

band order as the nature of each band determines the polarization property. Therefore, the valence-band order must be discussed. Figure 4 schematically depicts the band structures for (a) unstrained $Al_xGa_{1-x}N$, (b) strained $Al_xGa_{1-x}N$ on unstrained AlN, and (c) $Al_xGa_{1-x}N/AlN$ QWs. The $\boldsymbol{k}\cdot\boldsymbol{p}$ approach with the cubic approximation gives the energy separation between the upper Γ_7 and Γ_9 as

$$E(\Gamma_7) - E(\Gamma_9) = -\frac{\Delta' + \delta}{2} + \sqrt{\left(\frac{\Delta' + \delta}{2}\right)^2 - \frac{2}{3}\Delta'\delta}, \quad (1)$$

where $\Delta' = \Delta_{cr} + [D_3 - D_4(C_{33}/C_{13})]\varepsilon_{zz}$, δ is the spin-orbit splitting energy, D_i is the deformation potential, C_i is the elastic stiffness constant, and ε_{zz} is the strain tensor element along the c direction.[16] For AlN, $E(\Gamma_7) - E(\Gamma_9) > 0$ is satisfied due to the negative Δ_{cr}, and the resultant polarization is $\boldsymbol{E} \| c$, whereas for GaN, $E(\Gamma_7) - E(\Gamma_9) < 0$ and $\boldsymbol{E} \perp c$. For $Al_xGa_{1-x}N$, $E(\Gamma_7) - E(\Gamma_9)$ can be zero at a certain x (the critical Al composition), where the polarization switch occurs. As seen from Eq. (1), the condition of $E(\Gamma_7) - E(\Gamma_9) = 0$ corresponds to $\Delta' = 0$, and thus, the critical Al composition can be extracted assuming a linear relationship between the AlN and GaN parameters. Theoretical calculations[9,10] and a recent experiment[11] indicate that Δ_{cr} in AlN is around −220 meV. Therefore, −217 meV (Ref. 9) was used here, while the remaining parameters were from Ref. 13.

In unstrained $Al_xGa_{1-x}N$, the critical Al composition was estimated to be 0.044 from the condition of $\Delta_{cr} = 0$. For strained $Al_xGa_{1-x}N$ on unstrained AlN, the condition of $\Delta' = 0$ provided $x = 0.60$. This increase in the critical Al composition can be qualitatively understood by considering the effect of strain on each valence band. The in-plane compressive strain in $Al_xGa_{1-x}N$ pushes the $|X \pm iY\rangle$-related bands (Γ_9 and lower Γ_7) upward, but it is tensile strain along the growth direction which pushes the $|Z\rangle$-related band (upper Γ_7) downward, as schematically illustrated in Figs. 4(a) and 4(b). Consequently, the energy separation between the topmost Γ_7 and Γ_9 decreased, and then a larger Al composition was necessary for the polarization switch. It should be noted that 1-μm-thick $Al_xGa_{1-x}N$ on sapphire (0001) experimentally showed the polarization switch at $x = 0.25$,[14] implying the presence of residual compressive strain.

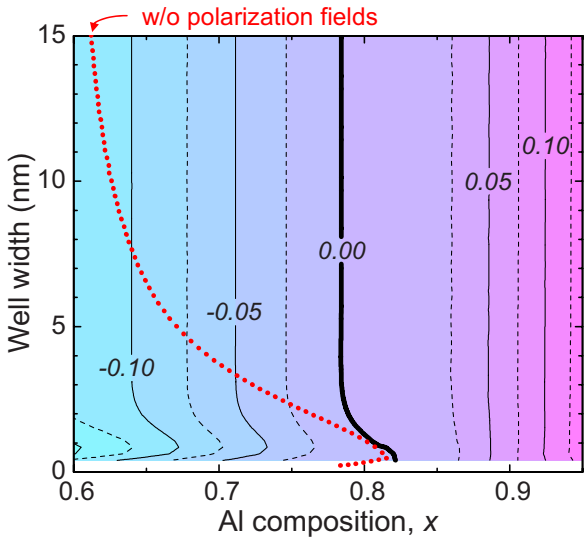

FIG. 5. (Color online) Contour plot of the calculated energy difference of $E(\Gamma_7^{QW}) - E(\Gamma_9^{QW})$ in the unit of electron volts. Red/gray dotted thick line is the $E(\Gamma_7^{QW}) - E(\Gamma_9^{QW}) = 0$ line for flat-band QWs without a polarization field, while (black) thick and thin lines are for QWs with polarization fields. The assumed spontaneous polarization was −0.040 C/m^2.

An additional factor that can affect the valence-band structure is quantum confinement. Because the hole effective mass at the topmost Γ_7 in AlN is much lighter than that at Γ_9 ($0.26m_0$ vs $3.57m_0$),[13] the energy of this Γ_7 is drastically lowered by quantum confinement. As drawn in Figs. 4(b) and 4(c), stronger confinement eventually causes the crossover between Γ_7 and Γ_9. In order to quantify the quantum confinement effect on the valence-band order, we numerically calculated the quantized level for the upper Γ_7 and Γ_9 in $Al_xGa_{1-x}N/AlN$ single QWs using a simple one-dimensional Schrödinger equation. The strain-dependent effective mass was assumed at Γ_7.[16] Figure 5 is the contour plot of the calculated energy difference between Γ_7^{QW} and Γ_9^{QW}, that is, $E(\Gamma_7^{QW}) - E(\Gamma_9^{QW})$. As mentioned above, $E(\Gamma_7^{QW}) - E(\Gamma_9^{QW}) = 0$ corresponds to the polarization switch. When the flat-band condition was assumed by neglecting the internal electric field, the critical Al composition for $E(\Gamma_7^{QW}) - E(\Gamma_9^{QW}) = 0$ in thicker QWs approached $x \sim 0.60$, as demonstrated by the (red/gray) thick dotted line in Fig. 5. This is reasonable because thicker QWs resemble strained thick layers where the critical Al composition was determined to be 0.60 using Eq. (1). However, thinner QWs moved the valence bands through quantum confinement as explained in Fig. 4, and consequently, Γ_9^{QW} could be the topmost valence band $[E(\Gamma_7^{QW}) < E(\Gamma_9^{QW})]$ even with Al compositions higher than ~0.60. Although this tendency qualitatively fits the experimental data shown in Fig. 3, it quantitatively does not.

Hence, we included the effect of the internal electric field caused by the spontaneous and piezoelectric polarizations. As reported for $In_yGa_{1-y}N$ and $Al_xGa_{1-x}N$ QWs many times, the electric field in the well region produces a triangular potential profile, which creates additional quantum confine-

ment and should promote the mechanism shown in Fig. 4(c). Because the reported spontaneous polarization in AlN spans a fairly broad range from −0.12 to −0.036 C/m^2, we treated this as a fitting parameter. Consequently, a value of −0.040 C/m^2 provided a good agreement between the experiment (Fig. 3) and calculation as indicated by (black) thick and thin lines in Fig. 5. Further decreasing the spontaneous polarization to the well-accepted −0.090 C/m^2 (Ref. 13) pushed the zero line up to $x \sim 0.85$. Therefore, as has occasionally been reported,[17–19] the spontaneous polarization in AlN is considered to be approximately −0.040 C/m^2, with which the internal electric field in $Al_{0.80}Ga_{0.20}N/AlN$ QWs, for example, was estimated to be −1.1 MV/cm, taking both spontaneous and piezoelectric polarizations into account. The internal electric field shifted the critical Al composition that satisfies $E(\Gamma_7^{QW}) - E(\Gamma_9^{QW}) = 0$ toward higher Al compositions, and the shift was more remarkable for thicker QWs. These findings can be interpreted as follows. For thin wells, the well width dominates the quantum confinement effect, and the internal electric field barely affects the critical Al composition. For thick wells, quantum confinement due to the well width becomes weak, whereas that due to the triangular potential well formed by the internal electric field remains. Thus, the critical Al composition for thicker QWs is determined by the internal electric field, independent of the well width.

Finally, we examined the reported optical polarization properties in $Al_xGa_{1-x}N$-based QWs. The c-oriented $Al_{0.66}Ga_{0.34}N/Al_{0.76}Ga_{0.24}N$ QWs on $Al_{0.86}Ga_{0.14}N$ (0.6 μm)/AlN (1.5 μm) templates showed $\boldsymbol{E} \| c$ polarization.[3,4] The well thickness was 5 or 10 nm. Although at first glance, the result seems to disagree with Fig. 5, it can be explained by (i) weak quantum confinement due to the relatively thick well width, (ii) weak quantum confinement due to the $Al_{0.76}Ga_{0.24}N$ barrier layer, and (iii) the weak internal electric field in the well due to the compensation with that in the $Al_{0.76}Ga_{0.24}N$ barrier layer; all of which may contribute to the promotion of $\boldsymbol{E} \| c$ polarization. Although the strain state seems complicated due to the presence of the 0.6-μm-thick $Al_{0.86}Ga_{0.14}N$ layer, our simple model predicted $E(\Gamma_7^{QW}) - E(\Gamma_9^{QW}) \sim 0$ for an $Al_{0.66}Ga_{0.34}N/Al_{0.76}Ga_{0.24}N$ QW coherently grown on AlN. This is the most extreme condition, and if the underlying $Al_{0.86}Ga_{0.14}N$ layer is (partially) relaxed, $\boldsymbol{E} \| c$ polarization is promoted; thus, there is a tolerable agreement between our model and the reported polarization.

In summary, we investigated the polarization properties of $Al_xGa_{1-x}N/AlN$ QWs. The emission with the polarization along $\boldsymbol{E} \perp c$ is observed up to $x \sim 0.82$, particularly for thinner QWs. This large Al composition for the polarization switch between $\boldsymbol{E} \perp c$ and $\boldsymbol{E} \| c$ is attributed to the in-plane compressive strain and the quantum confinement due to narrow wells and/or internal electric fields. The present results indicate that the appropriately designed c-oriented $Al_xGa_{1-x}N$ QWs can produce a surface emission even in the DUV spectral range, and may be a key in reconciling good crystalline qualities and emission properties.

The authors acknowledge K. Kojima and H. Kamon at Kyoto University for fruitful discussions.

*funato@kuee.kyoto-u.ac.jp
†kawakami@kuee.kyoto-u.ac.jp

[1] A. Khan, K. Balakrishnan, and T. Katona, Nat. Photonics **2**, 77 (2008).
[2] H. Hirayama, N. Noguchi, T. Yatabe, and N. Kamata, Appl. Phys. Express **1**, 051101 (2008).
[3] H. Kawanishi, M. Senuma, and T. Nukui, Appl. Phys. Lett. **89**, 041126 (2006).
[4] H. Kawanishi, M. Senuma, M. Yamamoto, E. Niikura, and T. Nukui, Appl. Phys. Lett. **89**, 081121 (2006).
[5] T. M. Al Tahtamouni, N. Nepal, J. Y. Lin, H. X. Jiang, and W. W. Chow, Appl. Phys. Lett. **89**, 131922 (2006).
[6] J. Shakya, K. Knabe, K. H. Kim, J. Li, J. Y. Lin, and H. X. Jiang, Appl. Phys. Lett. **86**, 091107 (2005).
[7] A. A. Yamaguchi, Phys. Status Solidi C **5**, 2364 (2008).
[8] M. Suzuki, T. Uenoyama, and A. Yanase, Phys. Rev. B **52**, 8132 (1995).
[9] S.-H. Wei and A. Zunger, Appl. Phys. Lett. **69**, 2719 (1996).
[10] J. Li, K. B. Nam, M. L. Nakarmi, J. Y. Lin, H. X. Jiang, P. Carrier, and S.-H. Wei, Appl. Phys. Lett. **83**, 5163 (2003).
[11] E. Silveira, J. A. Freitas, Jr., O. J. Glembocki, G. A. Slack, and L. J. Schowalter, Phys. Rev. B **71**, 041201(R) (2005).
[12] Y. Taniyasu, M. Kasu, and T. Makimoto, Appl. Phys. Lett. **90**, 261911 (2007).
[13] I. Vurgaftman and J. R. Meyer, J. Appl. Phys. **94**, 3675 (2003).
[14] K. B. Nam, J. Li, L. Nakarmi, J. Y. Lin, and H. X. Jiang, Appl. Phys. Lett. **84**, 5264 (2004).
[15] R. G. Banal, M. Funato, and Y. Kawakami, Appl. Phys. Lett. **92**, 241905 (2008).
[16] S. L. Chuang and C. S. Chang, Phys. Rev. B **54**, 2491 (1996).
[17] M. Leroux, N. Grandjean, J. Massies, B. Gil, P. Lefebvre, and P. Bigenwald, Phys. Rev. B **60**, 1496 (1999).
[18] S.-H. Park and S.-L. Chuang, Appl. Phys. Lett. **76**, 1981 (2000).
[19] S. P. Łepkowski, H. Teisseyre, T. Suski, P. Perlin, N. Grandjean, and J. Massies, Appl. Phys. Lett. **79**, 1483 (2001).